DEUTSCHES ELEKTRONEN-SYNCHROTRON DESY

DESY SR-80/16
October 1980

FREE EXCITON ENERGY TRANSFER IN Kr-Au SANDWICHES

by

N. Schwentner, G. Martens
Institut für Experimentalphysik der Universität Kiel

H. W. Rudolf
Sektion Physik der Universität München

NOTKESTRASSE 85 · 2 HAMBURG 52

To be sure that your preprints are promptly included in the
HIGH ENERGY PHYSICS INDEX ,
send them to the following address (if possible by air mail) :

DESY
Bibliothek
Notkestrasse 85
2 Hamburg 52
Germany

DESY SR-80/16
October 1980

Free Exciton Energy Transfer In Kr-Au Sandwiches

N. Schwentner (a), G. Martens (a) and H.W. Rudolf (b)
Institut für Experimentalphysik der Universität Kiel (a),
Sektion Physik der Universität München (b)

Subject classification: 13.5.1, 14.3.1, 17, 23

The photoelectron yield of Kr-Au sandwiches caused by energy transfer of Kr excitons to the Au substrate has been measured. The range for energy transfer of Kr excitons has been determined from the dependence of the yield on the thickness of the Kr overlayer for several excitation energies within the n = 1, n' = 1 and n = 2 exciton bands. The derived diffusion lengths of free excitons depend strongly on the individual exciton state and increase monotonically with the exciton energy within one exciton band as well as to higher exciton states from 30 Å for the n = 1 up to 300 Å for the n = 2 excitons. The efficiency for electron emission due to exciton decay exceeds the usual photoelectron yield of Au by a factor of 10.

Die durch den Energieübertrag von Kr Exzitonen auf die Au Unterlage bewirkte Photoelektronenausbeute von Kr-Au Schichtsystemen wurde gemessen. Die Reichweite für den Energieübertrag von Kr Exzitonen wurde aus der Abhängigkeit der Ausbeute von der Dicke der Kr Deckschicht für mehrere Anregungsenergien innerhalb der n = 1, n' = 1 und n = 2 Exzitonenbanden bestimmt. Die ermittelten Diffusionslängen der freien Exzitonen sind stark vom jeweiligen Exzitonenzustand abhängig und nehmen monoton mit der Exzitonenenergie sowohl innerhalb eines Exzitonbandes als auch zu höheren Exzitonenzuständen hin zu, ausgehend von 30 Å für die n = 1, bis zu 300 Å für die n = 2 Exzitonen. Die Effizienz der Elektronenemission durch den Zerfall von Exzitonen übersteigt die normale Photoelektronenausbeute von Au um einen Faktor 10.

submitted to: phys. stat. sol.

Introduction:

A theory of exciton-phonon coupling predicts for rare gas solids a coexistence of free and selftrapped excitons (1). In some luminescence experiments emission of free excitons has been identified for Xe, Kr and Ar besides the well known emission of selftrapped excitons (2,3,4). The intensity ratio of emission from free excitons and selftrapped excitons of about 10^{-3} is surprisingly low compared with the expectance of stable or at least metastable free excitons (1) and compared to the large barriers for selftrapping (3). Evidently the rate constants for radiative decay (2,4,5) of 10^6 to 10^9 (s^{-1}) are too small to compete effectively with selftrapping. Photoelectron yield experiments (6) have shown that energy transfer from rare gas matrices to rare gas guest atoms is fast enough to compete with selftrapping. In solid Xe, Kr and Ar selftrapping leads to excimer like centers similar to the free R_2^* excimers (2,3,4,7). The energy of these centers is lower by the amount of the excimer binding energy of 0.5 - 1 eV than that of the lowest free exciton states (fig. 1). Therefore the free and the localized states can be easily distinguished by their energies (4,5,7). Utilizing this energy difference it has been demonstrated by photoelectron energy distribution measurements (8) on Xe doped Ar matrices, that indeed energies of free excitons (fig. 1) are transfered. Furthermore it became clear that energy transfer can even compete with electronic relaxation within the higher free exciton states (8). Therefore one can hope to find a dependence of the transfer range on the primarily excited free exciton states in rare gas solids, whereas in the extensively studied systems of molecular crystals the interpretation usually starts from the electronically relaxed lowest singulet and triplet excitons (9).

We report on the transfer efficiency of different Kr excitons to a gold substrate versus Kr film thickness. The transfer efficiency is monitored by the amount of electrons emitted from the substrate through the Kr overlayer, thus exploiting the large penetration depth of low energetic electrons in rare gas films (10). A similar experiment has been reported for Xe

overlayers (11) but the quantum efficiency for the transfer was too low to analyse an energy dependence of the transfer range. From the energy dependence of the transfer range in Kr we are able to decide whether energy transfer only from selftrapped excitons or also from free or even from higher excited free exciton states takes place and if the transfer range is different for these exciton states. The experimentally determined parameters are not sufficient to intend a complete description of the transport mechanisms which has to be postponed until also the time dependence of the transfer processes has been studied.

Results:

Kr films have been condensed on a gold coated substrate cooled by a liquid He flow cryostat to about 10 K. The background pressure was well below 10^{-9} mb. The films have been excited by light from the synchrotron DESY in Hamburg which has been monochromatized with a resolution of 2 Å (about 20 meV at 10 eV). A LiF filter has been used to suppress higher order light. The film thickness has been monitored during deposition by measuring the interference fringes in the reflected light at a wavelength of 1400 Å. This wavelength is still in the transparent region of Kr and it is short enough to provide a sensitivity for thin Kr films of 10 Å and in general an accuracy of about 20 Å for the thickness. Photoelectrons emitted from the Au-Kr sandwhich have been collected by a grid and the current of the order of 10^{-11}A flowing to the substrate has been detected. More details are described elsewhere (8,12).

A representative collection of yield curves of a Kr-Au sandwhich in the range of the first excitons n=1, n'=1 and n=2 is shown in fig.2. Due to the normalization to the bare Au substrate yield the Au yield appears as a straight line with intensity 1. For very small film thickness of about 15 Å the positions of the prominent n = 1 and n' = 1 maxima are shifted by about 0.17 eV to lower energies (fig.3). These new maxima are attributed to surface excitons (14). They will be discussed after the analysis

of energy transfer processes in films with thickness d > 50 Å.

Intrinsic photoelectron emission from solid Kr should not occur for photon energies $\hbar\omega$ which are smaller than the vacuum level $\hbar\omega < E_G + E_A = 11.9$ eV, where E_G is the energy gap and E_A the electron affinity (15).

Other bulk effects like two photon excitations, exciton-exciton interactions and exciton enhanced impurity ionisation can be excluded for the range of fig.2 due to the low light intensity, the decrease of the yield with Kr film thickness and the purity of the samples as it has been discussed in (11). Therefore processes which are extrinsic concerning the Kr film are responsible for the yield in the whole spectral range shown in fig.2 and fig.3. The yield Y is composed of two interphase contributions (fig.4).

a) Electrons Y_{Au} from the gold substrate which have been excited by photons traversing the Kr film.
b) Electrons Y_{ET} from the gold substrate due to energy transfer from free or selftrapped excitons to the substrate.

A third contribution due to the decay of Kr excitons at the Kr surface is unprobable since the excitons are below the vacuum level. It could be easily identified since this contribution should remain up to large thickness. Fig.2 proves that it is either zero or so weak that it can be neglected for our discussion.

$$Y = Y_{Au} + Y_{ET} \qquad (1)$$

Y follows according to fig.4 from the incident light intensity I_o, the reflectivity R(d), the transmission of the Kr film, the quantum efficiency Q_{Au} of the substrate for photoelectron emission, the escape probability P(d) for electrons through the Kr films, the local density n(x) of photons absorbed in the film (i.e. the local density of produced excitons), the probability T(x) for energy transfer to the substrate due to an exciton created at the site x and the quantum efficiency Q_{ET} for electron emission from the substrate due to a transfered exciton. The reflectivity R is calculated from the exact expressions for a sandwhich (16) with the optical constants for

Kr (13) and for Au (17). n(x) is approximated by
$n(x) = (1-R)\ \mu \exp(-\mu x)$ with the extinction coefficient
$\mu = 4\pi k/\lambda$

$$Y_{Au} = I_o \quad (1-R(d)) \quad Q'_{Au} \quad P(d) \quad \exp(-\mu d) \qquad (2)$$

$$Y_{ET} = I_o(1-R(d)) \quad Q_{ET} \quad P(d) \quad \int_o^d \mu \exp(-\mu x) \quad T(x)\ dx \qquad (3)$$

For a comparison with fig.2 and fig.3 the yield Y has to be normalized to the substrate yield $Q_{Au} = Q'_{Au}\ (1-R(o))$ to obtain the relative yield Y_R

$$Y_R = (1-R(d))\ P(d) \quad \left[A\ B(d) + \exp(-ud)/(1-R(o))\right] \qquad (4)$$

with the ratio of the quantum efficiencies A

$$A = Q_{ET} / Q_{Au} \qquad (5)$$

and the energy transfer function B(d)

$$B(d) = \int_o^d \mu \exp(-\mu x)\ T(x)\ dx \qquad (6)$$

The escape probabilty P(d) follows immediately from the relative yield in the range from 8 eV to 9 eV where Kr is transparent (fig.2). The relative yields and thus also P(d) are constant in this range therefore they are used also for the whole range up to 11.5 eV. Now the interesting quantities A and B(d) can be extracted from the experimental results.

Discussion:

First we want to give some qualitative arguments which illustrate the final results. For a given thickness d and a fixed absorption coefficient the yield is mainly determined by A and B (equ.4). Therefore a comparison of the yield for different photon energies but with similar k values shows if A and B depend on photon energy i.e. the primary excited exciton state. We choose d = 345 Å and $0.3 \leq k \leq 0.4$ (fig.2 and insert). These k values appear at the low energetic flank of the n = 1 exciton (10.08 eV), on its high energetic flank (10.3 eV), on the low energetic flank of the n' = 1 exciton (10.7 eV), on its high energetic flank (10.95 eV)

and at the onset of the n = 2 exciton (11.15 eV). The corresponding relative yields are 0.5, 0.85, 1.35, 1.73, 2.3 (fig.2) which increase monotonically. This increase is general and does not depend on specially selected k values. It has to be attributed to an increasing A or B. Due to equ. 5 and since Q_{Au} is known to increase with the photon energy (18,19,20) we conclude that either the quantum efficiency Q_{ET} or the transfer efficiency B increase monotonically with the exciton energy. The memory of the transfer process on the primary exciton energy is the main result of these experiments. It shows that neither relaxation within the band of one exciton state nor electronic relaxation between different exciton states ($n = 2 \rightarrow n' = 1 \rightarrow n = 1$) nor selftrapping to excimer like centeres is completed before energy transfer. The shift of the maximum in the yield curves to larger film thicknesses for higher photon energies (fig.2) indicates that mainly the transfer range B increases with exciton energy.

These observations are substantiated by fits of the experimental curves with appropriate expressions for A and B. For B four different expressions have been used:

a) Diffusionmodel with diffusion length l and exciton density zero at the Kr/Au interface. In one version B_D^Q the exciton density is zero also at the Kr vacuum interface, which corresponds to surface quenching of excitons (11,21)

$$B_D^Q = \frac{\mu^2 l^2}{\mu^2 l^2 - 1} \quad \left\{ \frac{1}{\sinh(d/l)} - \exp(-\mu d)\left(\mu l + \frac{1}{\tanh(d/l)}\right)\right\} \qquad (7)$$

b) In the second version B_D^R the gradient of the exciton density is zero which corresponds to exciton reflection at the vacuum interface (11,21)

$$B_D^R = \frac{\mu^2 l^2}{\mu^2 l^2 - 1} \quad \left\{ \frac{1}{\cosh(d/l)} - \exp(-\mu d)\ \left(1 + \frac{\tanh(d/l)}{\mu l}\right)\right\} \qquad (8)$$

c) Förster-Dexter model (11,22) with an effective transfer radius d_F for a planar geometry:

$$B_F = \mu \int_o^d \exp(-\mu x)/(1+((d-x)/d_F)^4)\ dx \qquad (9)$$

d) The model for a dipol in front of a metallic mirror (23) with an effective transfer radius d_C

$$B_C = \mu \int_0^d \exp(-\mu x)/(1+((d-x)/d_C)^3)\, dx \qquad (10)$$

The thickness dependence has been fitted with a least square fit programm for fixed photon energies. The fits have been repeated for all photon energies between 10.00 eV and 11.3 eV with steps in the photon energies of 50 meV resulting in 26 points for A and B for each type of transfer expression. In a first run the quantum efficiency Q_{ET} and the transfer range parameter (either 1 or d_F or d_C) have been treated as free fitting parameters. Q_{Au} is needed for the fit. Krolikowski and Spicer observed a nearly linear increase of Q_{Au} from 0.005 (electrons/photon) at 9 eV to 0.015 at 11 eV (19). A similar dependence but an approximately 3 times larger absolute Q_{Au} has been reported by Samson (18) and by us (20). The evaluation is not sensitive to the absolute value of Q_{Au}, except for the absolute value of Q_{ET}, therefore the photon energy dependence also of Q_{ET} (equ.5) will be reliable but the absolute value may be uncertain by a factor of 3. We prefer the higher value because it has been obtained for comparable conditions.

From the fits we derive that Q_{ET} is independent on photon energy and that it is 10 times larger than Q_{Au} at 10.5 eV. A lower limit of Q_{ET} is 0.12 (electrons/exciton) and a more probable value is 0.36 (electrons/exciton). Furthermore surface quenching can be excluded since the fits with B_D^Q result in significantly higher deviations than with the other expressions.

In a second run the fits have been repeated with a fixed $Q_{ET} = 10 \quad Q_{Au}(\hbar\omega = 10.5$ eV). The results for the energy dependence of the diffusion lengths l (for B_D^R) and for the effective transfer radius d_F (for Q_F) are shown in fig.5. Both transfer ranges ($\mathbf{l}$,d_F) increase monotonically with the exciton energies as expected. There is no significant structure in the spectra of l and d_F which can be correlated to the individual exciton state. The scattering in neighbouring points of the spectra

reflects the uncertainities in the experimental spectra, the optical constants and the change of the optical constants with thickness (surface exciton) for the lowest thickness. The dashed diagonals in fig.5 serve as guidelines to indicate the trend. Fits of the relative yield with B_D^R for the thickness dependence are shown in fig. 6 for the four photon energies discussed before. The increase in yield intensity and diffusion length for d = 345 Å is significant. The low value for $\hbar\omega$ = 11.15 eV at d = 55 Å has to be attributed to the uncertainties above mentioned. The quality of the fits (B_D^R) is illustrated in fig.7 for the most significant thickness d = 345 Å and for d = 55 Å.

Conclusion:

The selftrapped excitons observed in luminescence are the final stage for almost all excitons before radiative decay occurs if they have not been quenched nonradiatively. Therefore there will be a contribution of these selftrapped excitons to energy transfer for all excitation energies. The selftrapped excitons are localized by a rearrangement of neighbouring atoms to an excimer like center with a reduced nearest neighbour distance (3,4,7). These centers are similar to "guest molecules" in a transparent medium due to the localization and the reduction in energy. For such a system a Förster-Dexter type description of energy transfer from localized centers to a plane is appropriate (equ. 9). Their contribution to the transfer range has to be independend on excitation energy because it starts from relaxed centers. If there is such a contribution than the small values of d_F of about 20 - 60 Å at the onset of the lowest exciton at 10 eV can be identified with this Förster-Dexter type of transfer. In the expressions given by Chance et al. (23) (equ. 10) which have been proven to be valid down to thicknesses below 10 Å (24) the integration concerning also the depth of the plane to which energy is transfered has been included. Besides this correction both formalisms represented by equ.9 and 10 are equivalent. Also the fit with equ. 10 agrees within 10 % with the results of equ.9. For isotropic excitation and a radiative quantum efficency q

(for a Kr film without substrate) the transfer range d_c in equ. 10 can be calculated (23) by

$$d_c = (\lambda^3 q\, n_{Au} k_{Au})^{1/3} (8\pi^3 n_{Kr} |\varepsilon_{Au} + \varepsilon_{Kr}|^2)^{-1/3} \qquad (11)$$

With $q = 1$ and the optical constants $n_{Au} = 1.25$, $k_{Au} = 1$, $\varepsilon_{Au} = 0.56 + i\,2.5$, $n_{Kr} = 1.4$, $\varepsilon_{Kr} = 1.96$ and the emission wavelength $\lambda = 1470$ Å a transfer range $d_c = 97$ Å is obtained. This value is larger than the result of a fit with equ. 10 of $20 \leq d_c \leq 60$. The difference can be attributed to a branching of the selftrapped exciton states (fig.1) into singulet and triplet states (4,5) with an intensity ratio of 0.02 (25) for the probably similar case of liquid Kr. If only singulet excitons contribute to the dipol-dipol energy transfer than a transfer range $d_c = 26$ Å is derived for the corresponding $q = 0.02$ in agreement with the experimental result.

The increase of the transfer range with excitation energy indicates a contribution to energy transfer from exciton states before selftrapping. Now a two step process with coherent and/or noncoherent migration of the excitation energy in the resonant exciton states and subsequent energy deposition has to be considered in addition to the transfer from excitons which survived long enough to become localized. The transfer of free excitons is described by a diffusion length l. Coherent and noncoherent migration can contribute to the diffusion conetant D (9,26).

$$l = \sqrt{D\tau}$$

τ means the free exciton lifetime which is expected to be three to four orders of magnitudes lower than the radiative lifetimes of the selftrapped states of 10^{-6} - 10^{-9} s (2,3,4).

The essential point is the monotonic increase of l within one exciton band and also in going to higher exciton bands. Within one band the lifetime may increase since more energy has to be dissipated before the exciton is in thermal equilibrium with

the lattice and before selftrapping starts. Also the diffusion constant may vary for excitons with larger wave vectors and larger group velocities at higher energies in the band. The increase of l to higher exciton states can be caused by a larger τ when the times for electronic relaxation from $n = 2 \rightarrow n' = 1 \rightarrow n = 1$ are spent as free excitons. Finally higher exciton states with a larger spatial extent may have also larger D values. A quantitative description of the free exciton mean free path and diffusion length is complicated by the fact that intraband scattering and also interband scattering (27,28) in the set of exciton bands displayed in fig.1 has to be considered. Furthermore the commonly used approximation of parabolic exciton bands (27,28) cannot be used throughout the whole range of the free exciton bands as is well known for the exciton bands of rare gas solids (28,29) and as is evident from fig.1. The Lorentzian line shapes of the n = 1 excitons of Kr(as well as Xe and Ar) observed in absorption experiments (14) indicate that these excitons belong to the class of weak exciton phonon coupling according to Toyozawa's classification (1). Lifetimes of the excitons of some 10^{-14} s due to exciton phonon scattering have been derived from the experimental halfwidth (14). Fugol' (3) estimated scattering times of 10^{-10}s - 10^{-11}s for thermal excitons near the bottom of the exciton bands which are much larger than those calculated from the linewidth. With these long lifetimes very large mean free path's for electron phonon scattering of several thousand Å have been predicted (3). The experimental l values have been attributed (3) to a more efficient localization with a localization time $\tau_{loc} \approx 10^{-12}$s and to scattering at grain boundaries separated by distances $z \approx 100$ Å. The diffusion length l has been calculated from $l = \sqrt{v z \tau_{loc}}$ with $v = \sqrt{2E_{kin}/m}$ for an exciton with group velocity v and kinetic energy E_{kin}. The diffusion length of fig. 5 can only be poorly approximated by this expression for the n = 1 exciton band extending from 10 eV to 10.5 eV with $z\tau_{loc} = 10^{-11}$cm s and a constant effictive mass m = 2.6 in units of the free electron mass (3). The above mentioned approximation of parabolic exciton bands has been used for these estimates (3).

The large quantum efficiency Q_{ET} compared to Q_{Au} is due to the surface sensitivity of the exciton decay at the substrate. This process is similar to electron emission from the decay of excited metastable rare gas atoms at metal surfaces since the energies are comparable (Kr $^3P_2$ = 9.92 eV; $^3P_0$ = 10.56 eV). The efficiencies in the case of Kr are not very accurate. For Kr $^3P_0$ a value of 0.25 (electron/metastable atom) has been reported (30) which is similar to $0.12 \leq Q_{ET} \leq 0.36$. Recently the dominating role of Penning ionisation compared to Auger like processes has been established by energy distribution measurements of the emitted electrons for Ne at Pd surfaces (31).

The transport of exciton energy has been studied earlier by an extensive investigation of the influence of surface contamination on photoluminescence excitation spectra of thick Kr films (34). The experimentally observed quenching of photoluminescence for excitation in the region of the n = 1 and n' = 1 exciton bands has been analysed by expressions similar to equ. 7,8 and 9 but with more general boundary conditions. These boundaries conditions include also intermediate cases between exciton reflection and complete quenching. A fit of the spectra for clean surfaces requires exciton reflection as boundary condition (34) in agreement with our results. The question if the energy transfer is due to exciton diffusion or due to dipol-dipol interaction between the exciton and the contamination layer could not be answered by these photoluminescence experiments (34). The obtained mean diffusion length l = 200 Å for the region of n = 1 and n' = 1 excitons is consistent with our results (Fig.5). A comparison of the alternatively determined effective transfer radius d_F with d_C values discussed by us can be missleading because in our case the Au substrate is the partner for dipol-dipol interaction, whereas in the earlier work the partner is given by a contamination layer consisting of atomspheric gases with unknown composition. The assumption of a constant diffusion length (34) is not in agreement with our results. This discrepancy indiates that the present experiments are

more sensitive for the energy dependence of the diffusion length.

Finally the positions of the n = 1 and n' = 1 surface excitons of 10.02 and 10.70 ev (fig. 3) agree within our accuracy with surface excitons at 10.02 and 10.68 observed by Saile et al. (14). The shift relative to the bulk excitons is too large to be explained by the interaction with the gold substrate (32). The magnitude of the yield for d = 15 Å is a consequence of a transfer range of 20 Å - 50 Å and can be calculated from the bulk absorption coefficient shifting it by 0.1 to 0.2 eV to lower energies. The disappearance at large thicknesses will be due to a reduced transfer efficiency compared to bulk excitons since the surface excitons cannot penetrate into the film.

The experiments at the Deutsches Elektronen Synchrotron DESY in Hamburg have been supported by the DFG. We acknowledge the help of Dr. F.-J. Himpsel in the experiments and the support of Professor W. Steinmann.

References:

1) Y. Toyozawa in "Vacuum Ultraviolet Radiation Physics" eds. E.E. Koch, R. Haensel, C. Kunz, Pergamon Vieweg, braunschweig 1974, p. 317
E.I. Rashba, Izv. An SSR, Ser. Fiz. Ed. 40, 535 (1976)

2) F. Coletti, A.M. Bonnot, Chem. Phys. Letters 55, 92 (1978)
R. Kink, M. Selg, preprint (1979)
G. Zimmerer, J. Luminescence 18/19, 875 (1979)

3) I.Yu Fugol', Advances in Physics 27, 1 (1978)

4) N. Schwentner, E.E. Koch, J. Jortner in "Rare Gas Solids III" eds. M.L. Klein and J.A. Venables, Academic Press (1981)

5) N. Schwentner in "Luminescence of Inorganic Solids" ed. B. DiBartolo, Plenum Press, New York (1978)

6) Z. Ophir, B. Raz, J. Jortner, Phys. Rev. Letters 33,415 (1974)
Z. Ophir, B. Raz, J. Jortner, V. Saile, N. Schwentner, E.E. Koch, M. Skibowski, W. Steinmann, J. Chem. Phys. 62, 650 (1975)

7) J. Jortner in "Vacuum Ultraviolet Radiation Physics" eds. E.E. Koch, R. Haensel, C. Kunz, Pergamon Vieweg, Braunschweig (1974), p. 263

8) N. Schwentner, E.E. Koch, Phys. Rev. B 14, 4687 (1976)

9) H.C. Wolf in "Advances in Atomic and Molecular Physics" III ed. D.R. Bates, Academic Press (1967)
C. Powell, Z.G. Soos, J. Luminescence 11, 1 (1975)
R. Silbey, Ann. Rev. Phys. Chem. 27, 203 (1976)

10) N. Schwentner, Phys. Rev. B14, 5490 (1976)

11) Z. Ophir, N. Schwentner, B. Raz, M. Skibowski, J. Jortner, J. Chem. Phys. 63, 1072 (1975)

12) N. Schwentner, E.E. Koch, V. Saile, M. Skibowski and A. Harmsen in "Vacuum Ultraviolet Radiation Physics" eds. E.E. Koch, R. Haensel, C. Kunz, Pergamon Vieweg 1974, p.732

13) I.T. Steinberger, P. Maaskant, S.E. Webber, preprint submitted to J. Chem.Phys.

14) V. Saile and E.E.Koch, to be published

15) N. Schwentner, F.J. Himpsel, V. Saile, M. Skibowski, W. Steinmann, Phys. Rev. Letters 34, 528 (1975)

16) S.V. Pepper, J. Opt. Soc. Am. 60, 805 (1970)

17) J.J. Hagemann, J. Gudat, C. Kunz, J. Opt. Soc. Am 65, 742 (1975) and DESY SR-74/7

18) J.A.R. Samson in "Techniques of Vacuum Ultraviolet Spectroscopy", Wiley, New York (1967)

19) W.F. Krolikowski, W.E. Spicer, Phys. Rev. B1, 478 (1970)

20) E.E. Koch, F. Raz, V.Saile, N. Schwentner, M. Skibowski, W. Steinmann, Japan J. Appl. Phys. Suppl. 2 Pt. 2, 775 (1974)

21) D.M. Simpson, Proc. R. Soc. A 238, 402 (1957)

22) Th. Förster, Ann. Phys. 6, 55 (1948)
D.L. Dexter, J. Chem. Phys. 21, 836 (1953)

23) R.R. Chance, A. Prock, R. Silbey, J. Chem. Phys. 62, 2245 (1975)

24) A. Campion, A.R. Gallo, C.B. Harris, H.J. Robota and P.M. Whitmore, Chem. Phys. Letters 73, 447 (1980)

25) S. Kubota, I. Nishida and J. Raun, J. Phys. C, Solid State 11, 2645 (1978)

26) V. Brn, A. Suna, Y. Tomiewicz, P. Avakian, R.P. Groff, Phys. Rev. B 5, 5222 (1972)

27) Y. Toyozawa, Progr. Theoret. Phys. 20, 53 (1958)

28) R.S. Knox "Theory of Excitons", Academic Press New York (1963) p. 55

29) R.S. Knox, Phys. Chem. Solids 9, 265 (1959)

30) F.B. Dunning, R.B. Rundel, R.E. Stebbing, Rev.Sci. Instrum. 46, 697 (1975)

31) H. Conrad, G. Ertl, J. Küppers, submitted to Phys. Rev. Letters

32) R.R. Chance, A. Prock, R. Silbey, Phys. Rev. A 12, 1448 (1975)

33) A.G. Molchanov, Soviet Phys. Usp. 106, 165 (1972)

34) Ch. Ackermann, R. Brodmann, U. Kuhn, T. Suzuki, G. Zimmerer, phys. stat. sol. (b) 74, 579 (1976)

Figure captions

Fig. 1: Schematic exciton bands of solid Kr.
Left hand side: Energy of excimer type localized excitons versus internuclear separation r in analogy to estimates for solid Xe (33).
Right hand side: Free exciton bands versus wave vector k in analogy to the calculations for Ar (28,29) including experimental values (eg.14).

Fig. 2: Kr - Au sandwhich yield normalized to the Au substrate yield for 4 Kr thicknesses d. The positions of the n = 1, n' = 1 and n = 2 excitons are marked. The inset shows the absorption coefficient k of Kr (13).

Fig. 3: Comparison of normalized Kr - Au sandwhich yield for thicknesses of 15 Å (full curve) and of 55 Å (dashed curves, see fig. 2) in the region of n = 1, n' = 1 and n = 2 excitons.

Fig. 4: Scheme for the contributions Y_{Au} and Y_{ET} to the yield of a Kr-Au sandwhich with reflectivity R. The shaded beam indicates energy transfer by excitons, the straight beams the escape of the electrons and the wavy beams the light pass with incident intensity I_0.

Fig. 5: Lower part: Energy dependence of the diffusion length l (circles) and the effective transfer range d_F (crosses) (see text).
Upper part: Absorption coefficient k of solid Kr.

Fig. 6: Experimental yield (points) and corresponding fits (solid lines) for a set of photon energies where the absorption coefficients k of Kr are rather similar (see text). For the fits the optical constants for each photon energy have been used.

Fig. 7: Experimental yield (solid line, dashed line) and fit (circles, crosses) for a thickness d = 345 Å and d = 55 Å respectively with the l spectrum of fig. 5.

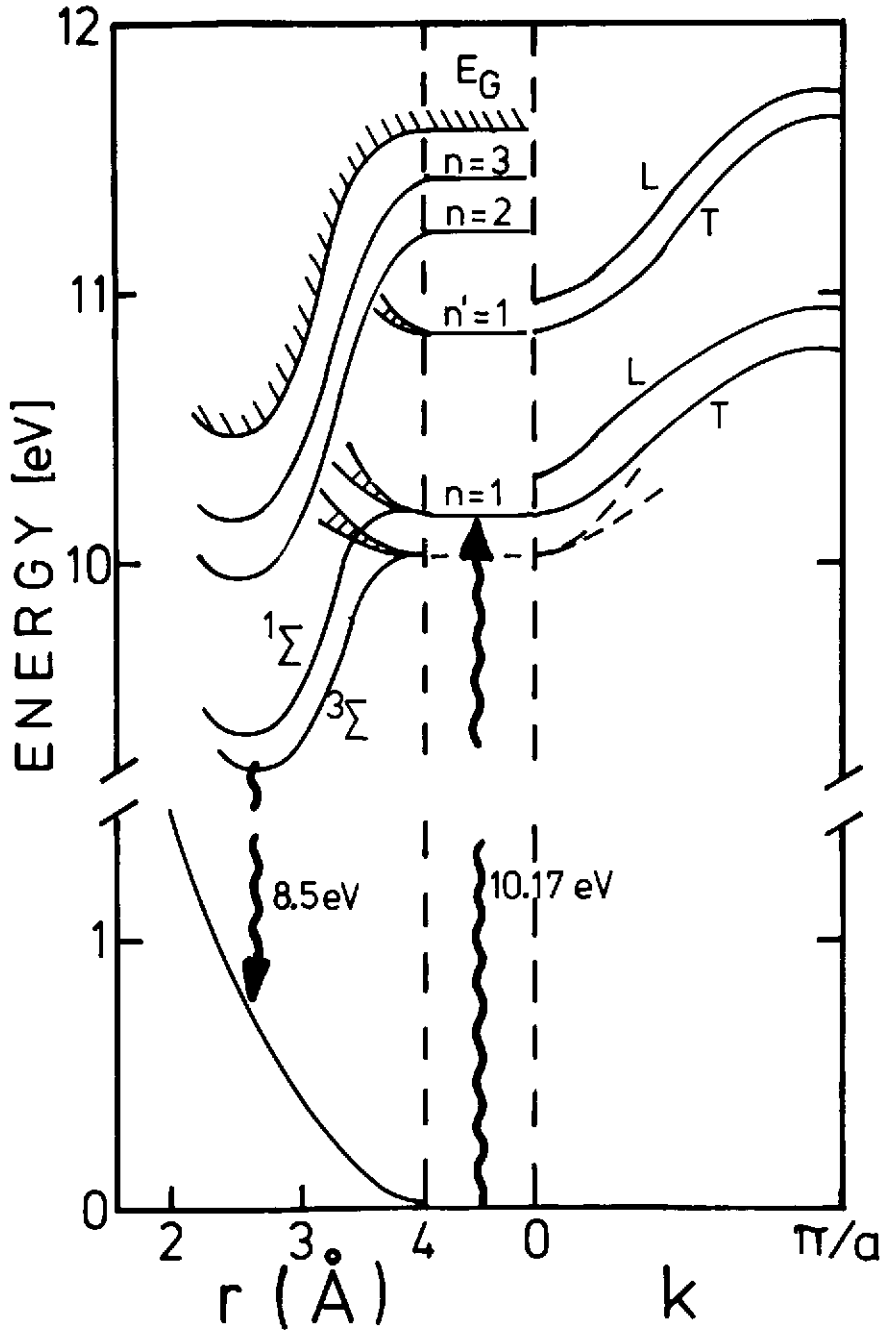
12
11
10
1
0
ENERGY [eV]
E_G
n=3
n=2
n'=1
n=1
L
T
L
T
$^1\Sigma$
$^3\Sigma$
8.5eV
10.17 eV
2
3
4
0
r (Å)
k
π/a

Fig. 1

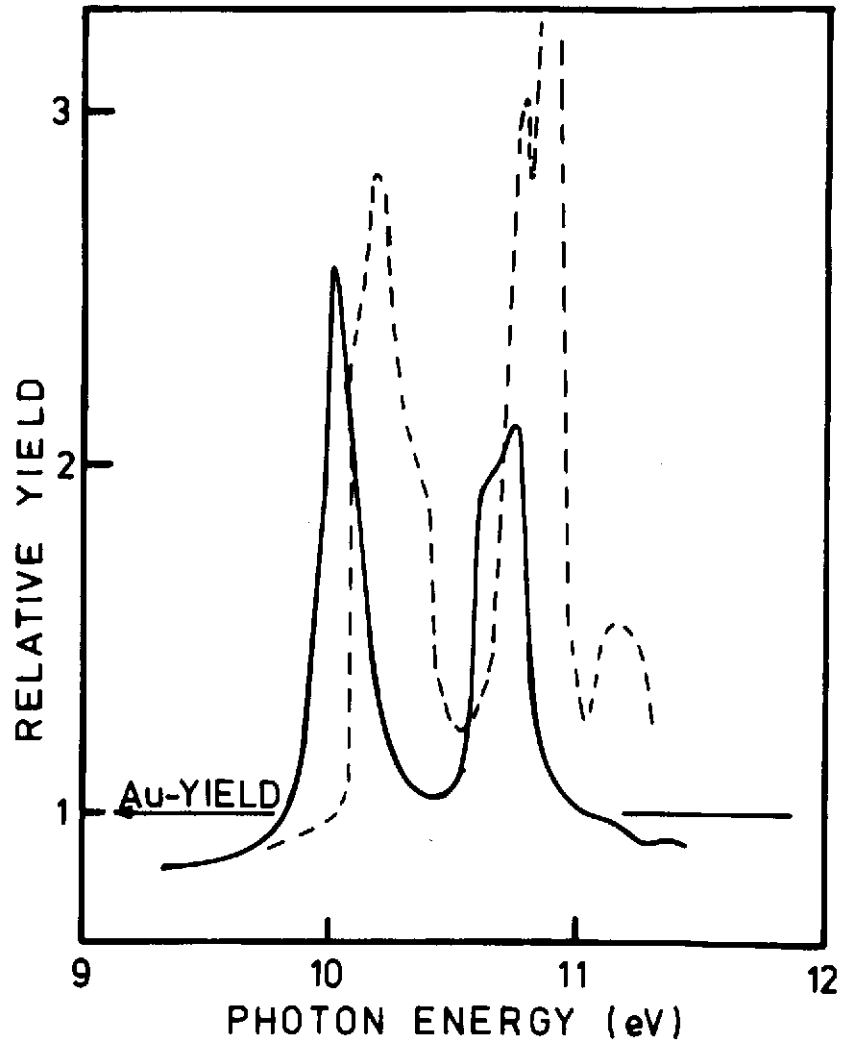
3
2
1
RELATIVE YIELD
Au-YIELD
9
10
11
12
PHOTON ENERGY (eV)

Fig. 2

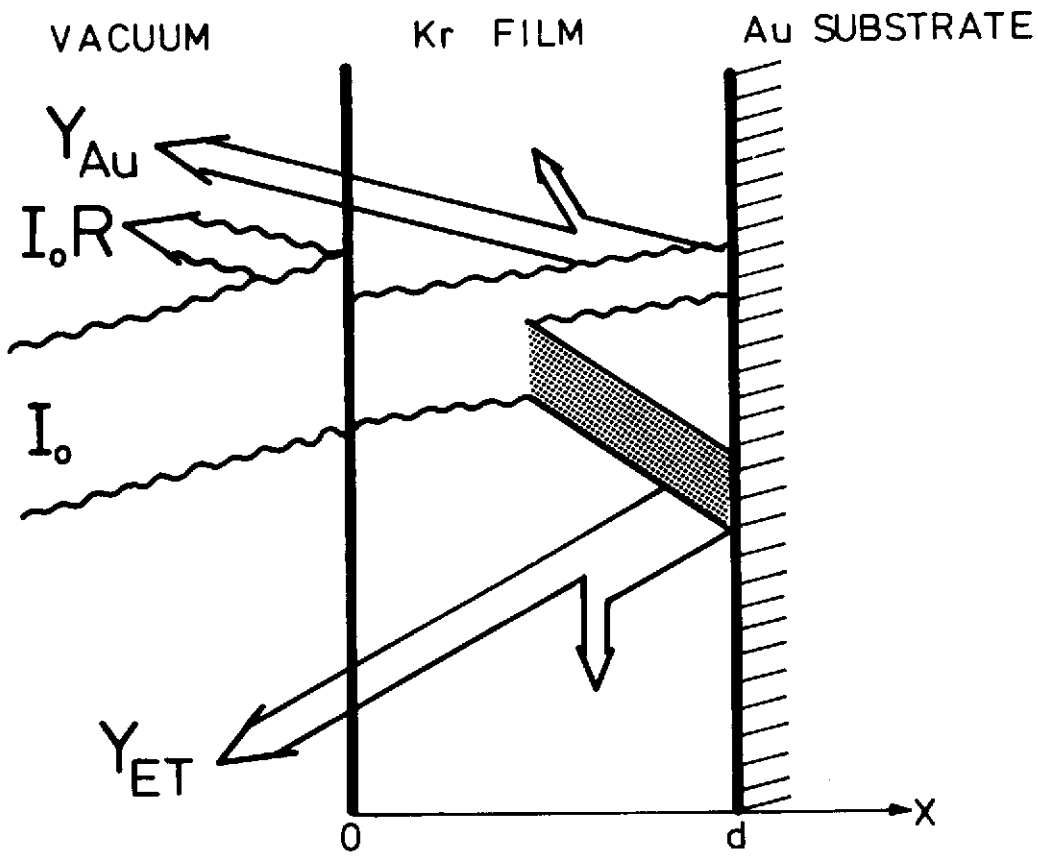
VACUUM
Kr FILM
Au SUBSTRATE
Y_{Au}
I_oR
I_o
Y_{ET}
0
d
X

Fig. 4

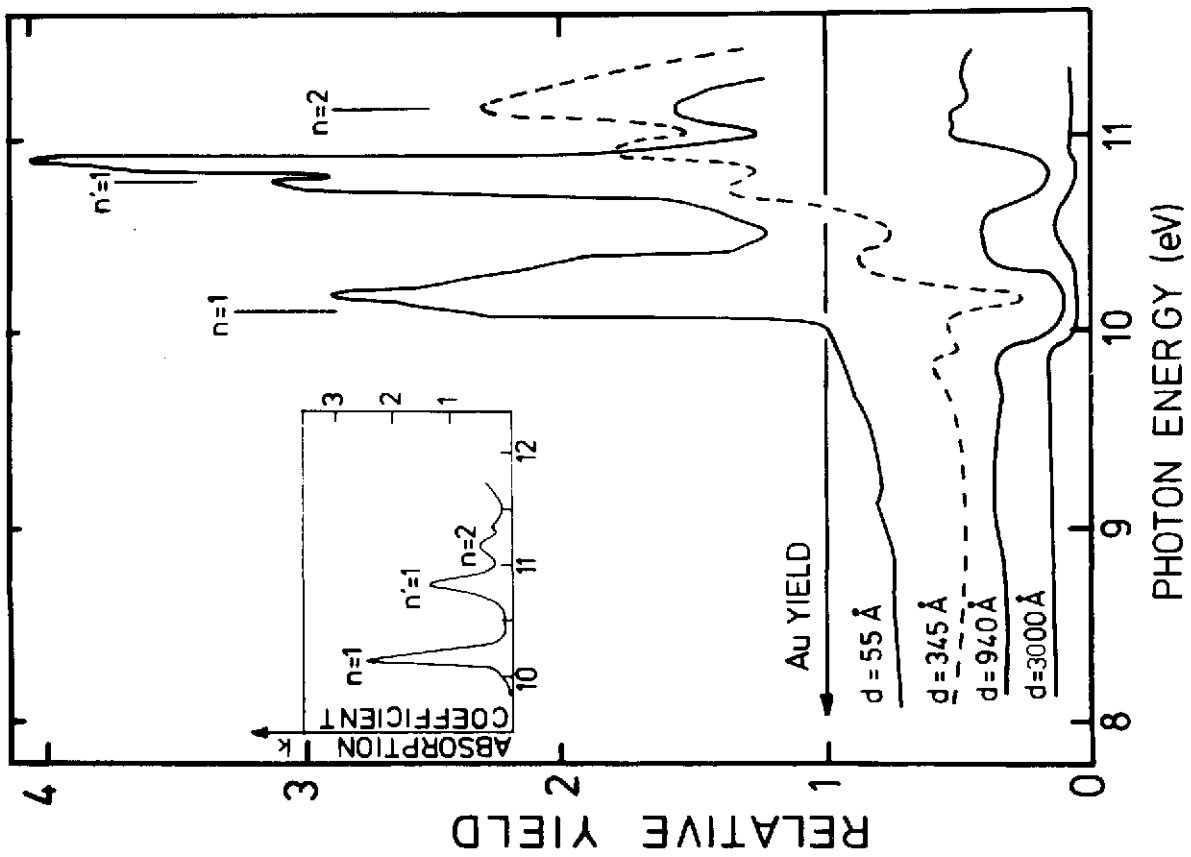
RELATIVE YIELD
PHOTON ENERGY (eV)
Au YIELD
d=55 Å
d=345 Å
d=940 Å
d=3000 Å
n=1
n=2
n'=1
ABSORPTION COEFFICIENT k

Fig. 5

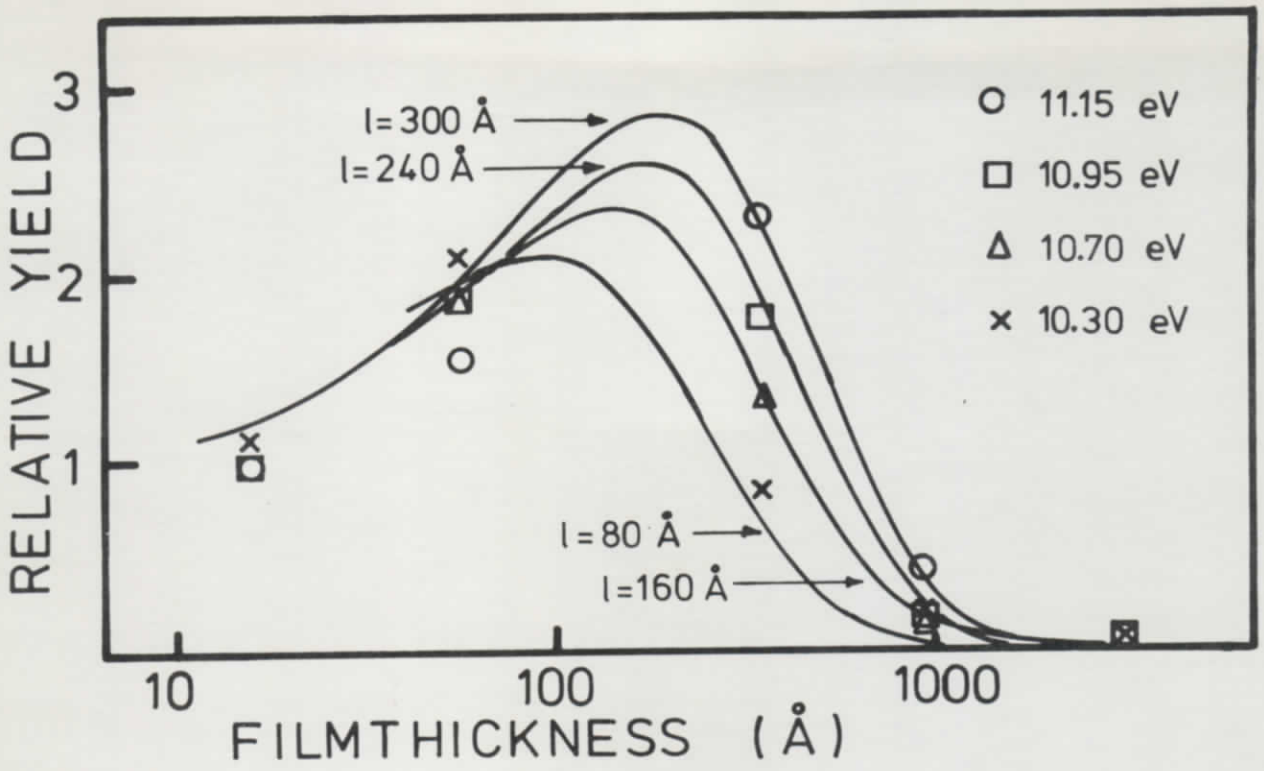
RELATIVE YIELD
FILMTHICKNESS (Å)
l = 300 Å
l = 240 Å
l = 80 Å
l = 160 Å
11.15 eV
10.95 eV
10.70 eV
10.30 eV

Fig. 6

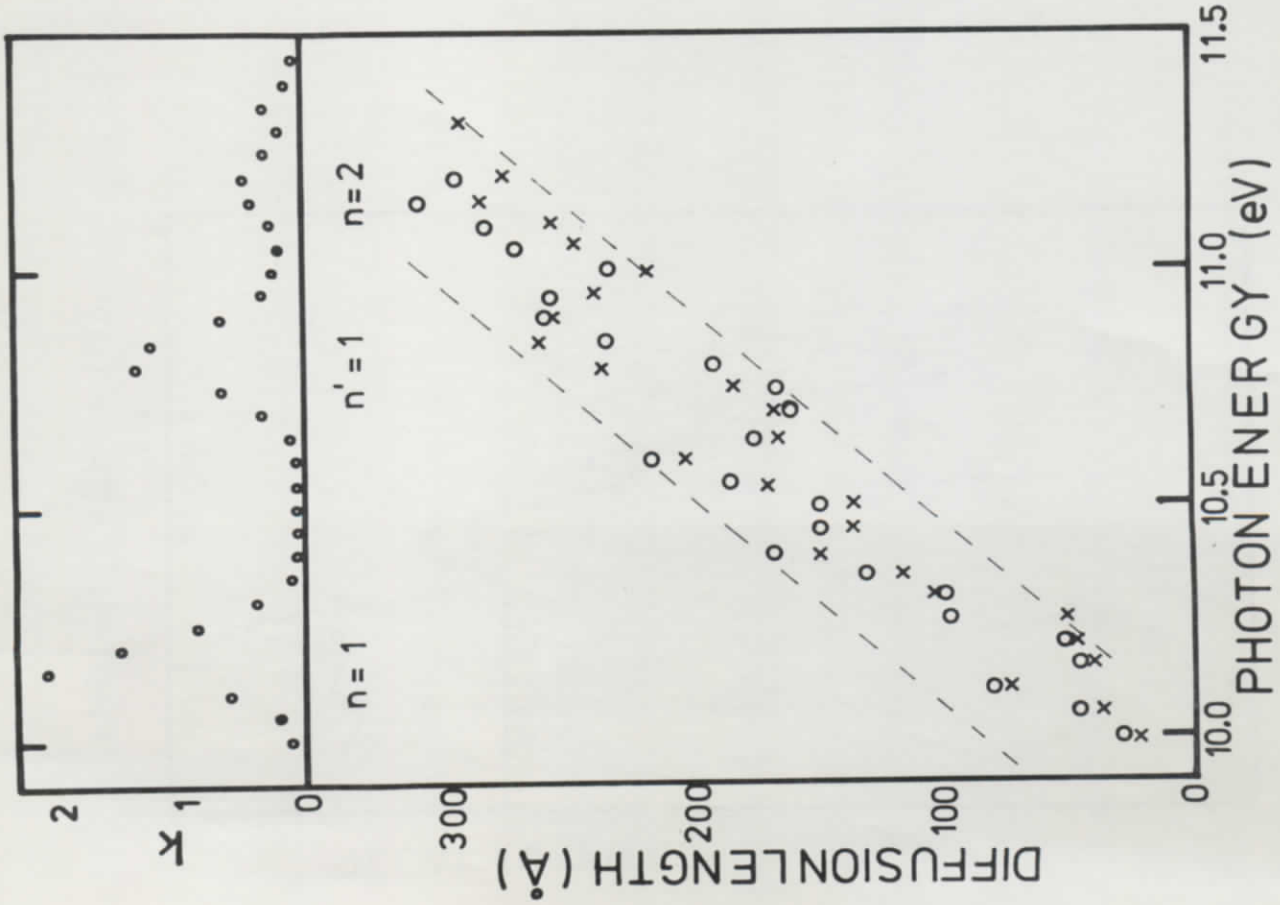
κ
DIFFUSIONLENGTH (Å)
PHOTON ENERGY (eV)
n = 1
n' = 1
n = 2

Fig. 5

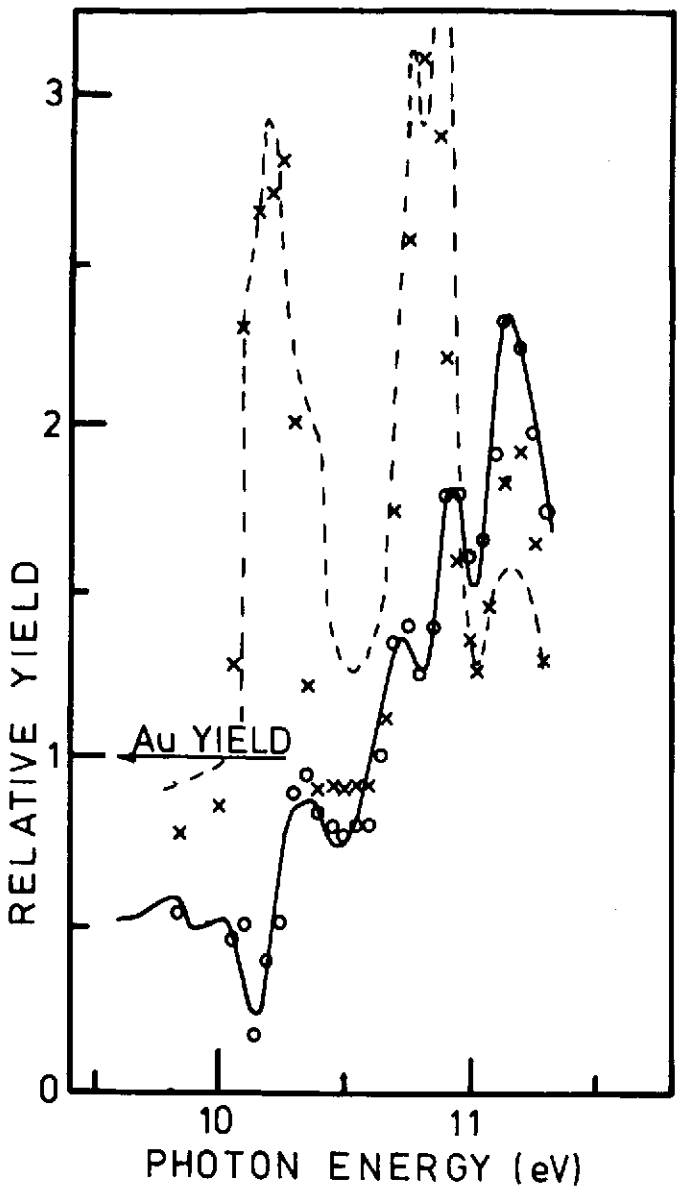

Fig. 7